



Necessity of Log(1/R) and Kubelka-Munk transformation in chemometrics analysis to predict white rice flour adulteration in brown rice flour using visible-near-infrared spectroscopy

Laila RAHMAWATI^{1*} , Aryanis Mutia ZAHRA², Riana LISTANTI³, Rudiati Evi MASITHOH², Hari HARIADI⁴, ADNAN⁴, Merynda Indriyani SYAFUTRI⁵, Eka LIDIASARI⁵, Rima Zuriah AMDANI¹, PUSPITAHATI⁶, Sri AGUSTINI⁷, Laela NURAINI⁴, Slamet Diah VOLKANDARI¹, Mohammad Faiz KARIMY¹, SURATNO¹, Anjar WINDARSIH¹, Muhammad Fahri Reza PAHLAWAN²

Abstract

This study compared the calibration model performance of reflectance to absorbance transformation spectra combined with pre-processing spectra to find the best model to predict white rice flour adulteration in brown rice flour using the visible and near-infrared spectrometer. Partial least squares regression (PLSR) and principal component regression (PCR) were compared using reflectance, Kubelka-Munk (KM), and Log(1/R) spectra. Area normalization (AN) and Savitsky-smoothing Golay's (SGS) were pre-processing methods. The sample was white rice flour mixed with brown rice flour at 0%, 5%, 10%, 15%, 20%, and 25%. Reflectance spectra outperformed KM and log (1/R) spectra in this study. Reflectance spectra provided the best model for PLSR and PCR. Pre-processed SGS spectra were best for PLSR, while raw reflectance spectra were best for PCR. PLSR and PCR both had an R² of prediction of 0.96, while the overall average R² of prediction favors PLSR over PCR. The present study led to the discovery of a simple novel method for developing adulteration flour and showed that a visible near-infrared spectrometer combined with PLSR, or PCR, could predict white rice flour adulteration in brown rice flour.

Keywords: Kubelka-Munk; spectra transformation; pre-processing; chemometrics; multivariate analysis.

Practical Application: A rapid and non-destructive measurement to predict the adulteration of rice flour by visible near-infrared spectroscopy.

1 Introduction

Spectroscopy is a method that studies the interaction between electromagnetic waves with matter (van der Meer, 2018). Various studies have proven that spectroscopy can measure postharvest product parameters (Jaiswal et al., 2014; Jie et al., 2014; Laborde et al., 2021; Masithoh et al., 2020a; Santos et al., 2013; Walsh et al., 2020). Depending on the electromagnetic waves used, spectroscopy can be divided into ultraviolet (UV) spectroscopy, which uses ultraviolet light (100-400 nm); visible (Vis) spectroscopy which uses visible light (400-700 nm); Infrared (IR) spectroscopy which uses infrared light (700 nm-1mm). Spectroscopy in the infrared region could be divided into near-infrared (700-2500 nm), mid-infrared (2500-25000nm), and far-infrared (25000nm-1mm). The different electromagnetic waves can determine what product and parameter can be measured.

The use of spectroscopy to analyze the quality parameters of powdered products has been widely reported. Adulteration detection in powder products could be detected using NIR

(Quelal-Vásconez et al., 2018, 2019; Rismiwandira et al., 2021; Xu et al., 2013) and MIR (Masithoh et al., 2022; Rodríguez et al., 2019; Roosmayanti et al., 2021). The chemical parameter of powdered product could also be quantified using NIR spectroscopy (Masithoh et al., 2020b; Veselá et al., 2007; Wu et al., 2008) or MIR spectroscopy (Masithoh et al., 2022; Quelal-Vásconez et al., 2018, 2019; Rodríguez et al., 2019; Roosmayanti et al., 2021; Xu et al., 2013). Adulteration detection in powder products is related to food authentication to minimize food fraud. Food adulteration will affect the physicochemical properties of the product, physical characteristics, sensory, presence of bioactive compounds, and a food allergen, which is related to the right of consumers to guarantee food safety, quality, and authenticity. Vis-NIR spectroscopy will enhance the method of classifying food products (Chen et al., 2006; Cruz, 2007; Rahmawati et al., 2022; Zhang et al., 2023; Zhou et al., 2023) and identifying the quality parameters of powder products as a way of smart authentication (Masithoh et al., 2022; Quelal-Vásconez et al.,

Received 02 Nov., 2022

Accepted 21 Dec., 2022

¹Research Center for Food Technology and Processing, National Research and Innovation Agency, Yogyakarta, Indonesia

²Department of Agricultural and Biosystems Engineering, Faculty of Agricultural Technology, Universitas Gadjah Mada, Yogyakarta, Indonesia

³Department of Agricultural Technology, Faculty of Agriculture, Universitas Jendral Soedirman, Central Java, Indonesia

⁴Research Center for Appropriate Technology, National Research and Innovation Agency, West Java, Indonesia

⁵Department of Agricultural Technology, Faculty of Agriculture, Universitas Sriwijaya, South Sumatera, Indonesia

⁶Department of Agricultural Engineering, Faculty of Agriculture, Universitas Sriwijaya, South Sumatera, Indonesia

⁷Research Center for Agroindustry, National Research and Innovation Agency, Banten, Indonesia

*Corresponding author: laila.rahmawati53@gmail.com

2018, 2019; Rodríguez et al., 2019; Roosmayanti et al., 2021; Xu et al., 2013).

Vis-NIR Spectroscopy uses light in the visible and near-infrared regions to measure product parameters. The light emitted by the source onto the product's surface will be reflected, transmitted, or absorbed by the molecules in the product (Guo et al., 2016). The amount of reflected, transmitted, or absorbed light in a range of wavelengths is called spectra. The spectra contain information related to the chemical and physical parameters of the product (Juhász et al., 2005). Spectra in the visible light region contain information on color pigment. In contrast, NIR spectra contain information related to interactions between electromagnetic light with C-H-O-N molecules (Xie et al., 2009). Chemometrics analysis involves extracting information within the spectra to identify desired quality parameters.

Chemometrics analysis of spectra consists of two critical steps, i.e., pre-processing spectra and calibration modeling. Spectra pre-processing is necessary to reduce trivial information within the spectra (scattering, noise, baseline correction) and amplify the critical signal for measurement (Mishra et al., 2020). Calibration modeling is the step to connecting the multiple variables of spectra with the desired quality parameter (Masithoh et al., 2020b). Two typical calibration modeling methods were partial least squares regression (PLSR) and principal component regression (PCR). The combination of calibration modeling and pre-process spectra dramatically determine the model's performance to predict desired quality parameters using spectra. Several spectra pre-processing methods often used include normalization, standard normal variate, smoothing, Savitsky-Golay's derivative, and multiple scatter correction. Suitable pre-process spectra could improve model performance (Mishra et al., 2021). However, spectra pre-processing can also have a negative impact on the model performance (Schoot et al., 2020). Therefore, a comparison of model performance built from several pre-process spectra must be made to find a model with the best prediction performance.

Pre-process spectra could be applied directly to reflectance or transmittance spectra. Considering that the light absorbed by the molecules is essential information, several studies have transformed the reflectance or transmittance spectra into absorbance spectra before creating a calibration model. The absorbed light is essential because it can cause interactions in the product molecules or excitation, such as stretching, twisting, rocking, wagging, scissoring, and so forth (Nielsen, 2017). Absorbance (A) spectra could be quantified using Beer's Law, that is, $A = \log(1/T)$ for transmittance mode and $A = \log(1/R)$ for reflectance mode (Schaare & Fraser, 2000). In addition, the Kubelka-Munk equation ($A = (1 - R^2)/2R$) can also be used for reflectance spectra which also account for scattering (Nicolai et al., 2007a).

Each calibration model typically uses a single pre-process spectra. However, multiple pre-process spectra can also be carried out to better model performance (Mishra et al., 2020). Several studies have proved that using multiple pre-process spectra could yield better model performance to identify adulterated samples (Quelal-Vásconez et al., 2018; Xu et al., 2013). However, to the best of our knowledge, a study regarding the necessity of transformation reflectance or transmittance spectra to absorbance combined

with pre-processing spectra for an adulterated sample has not been reported yet. Therefore, this study aimed to compare the calibration model performance of original reflectance, Log(1/R), and Kubelka-Munk Transformation spectra combined with pre-processing spectra to find which combination yielded the best model to predict adulteration of white rice flour in brown rice flour using the visible and near-infrared spectrometer.

2 Materials and methods

2.1 Samples

Brown rice flour and white rice flour were obtained from the local market in Yogyakarta, Indonesia. The flours were separately sieved with a 50-mesh sieve (0.29 mm, ASTM standard) to obtain uniform samples. The flour that did not pass the sieve was ground in a blender and re-sieved. Sieved brown rice flours were then intentionally mixed with white rice flour. The white flour in brown rice flour was 0%, 5%, 10%, 15%, 20%, and 25%, with each total mix of 30 grams. Adulterated flours were mixed manually in a closed bottle for minutes. The samples were dried using a food dehydrator at 60 °C for 12 hours to remove excess water.

2.2 Spectra acquisition

The spectrometer instrument used in this study was Vis-NIR miniature spectrometer (Flame-T-VIS-NIR Ocean Optics) equipped with a tungsten halogen lamp (360-2400 nm, HL-2000-HP-FHSA Ocean Optics) and a sensor probe (QR400-7-VIS-NIR Ocean Optics). For each adulteration percentage, 30 grams samples were divided into six samples of 5-gram flour. The sample was placed in a 2-centimeter-diameter, 1-centimeter-thick aluminum cup. Reflectance spectra were measured at a 90-degree angle to the sample's surface. For each sample, ten reflectance spectra were obtained. The total number of spectra obtained was six levels of adulteration with five samples and ten replication (n=300 spectra).

2.3 Chemometrics analysis

All reflectance spectra taken were compiled and transformed into absorbance in Ms. Excel. Reflectance to absorbance spectra was quantified using Equation 1, and Kubelka-Munk (KM) spectra were quantified using Equation 2. Spectra were imported into the Unscrambler® X software (CAMO, Oslo, Norway) for further chemometric analysis. Several pre-process spectra were applied to reflectance, log (1/R), and KM spectra, such as Savitsky-Golay's smoothing (SGS), area normalization (AN), standard normal variate (SNV), multiple scatter correction (MSC), Savitsky-Golay's first derivative (SGD 1st, polynomial=2, side points'32). Multivariate analysis principal component regression (PCR) and partial least squares regression (PLSR) were performed using spectra data as a predictor variable (X) and adulteration level as a dependent variable (Y). Before performing multivariate analysis, the dataset was divided into a calibration set (2/3 data, 200 samples) used to build the calibration model and a prediction set (1/3 data, 100 samples) used to test the model prediction performance.

$$A = \log\left(\frac{1}{R}\right) \quad (1)$$

$$KM = \frac{1 - R^2}{2R} \quad (2)$$

3 Results and discussion

3.1 Vis-NIR spectra of adulterated brown rice

Vis-NIR spectra of adulterated brown rice were measured at wavelength 345-1033 nm with an interval of 0.2 nm. Due to heavy noise appearing at <400 nm and >1000 nm, those spectra were excluded from the analysis (Figure 1). In the wavelength range of 400-1000 nm, the number of variables used was 3188 variables. Reflectance spectra obtained from the spectrometer were transformed using the Kubelka-Munk equation and log (1/R). The reflectance, KM transformed, and log (1/R) transformed spectra of adulterated brown rice.

Figure 1 shows that KM and Log(1/R) spectra have the opposite shape of the reflectance spectra. However, all three appear to have similar trend spectra between adulterated samples. Pure brown rice (0% adulteration) seems to have a higher absorbance than the adulterant sample. As the level of adulteration increases, the sample's absorbance appears to be getting lower. The higher

the level of adulteration, the brighter the sample will appear. The bright sample will have a higher reflectance, while the darker sample will have a higher absorbance.

The reflectance spectra, KM spectra, and Log(1/R) spectra of adulterated brown rice exhibit similar patterns of absorbance peaks. All three spectra show three pattern peaks at around 410 nm, 670 nm, and 990 nm. The peak at around 410 nm was influenced by the carotenoid pigment (Cortés et al., 2016), which are β -carotene and lutein (Lamberts & Delcour, 2008). The peak at around 670 nm was correlated with chlorophyll- α (Guo et al., 2016; Lichtenthaler & Buschmann, 2001). The second overtone of OH stretching affected the peak at around 990 nm (Fernández-Navales et al., 2019).

3.2 PLSR model

PLSR is a quantitative method used to connect multiple variables of spectra with the desired variable, in this case, adulterant concentration. PLSR will reduce spectra dimension and form new variables, up to 20, that can best explain the desired variable with minimal information loss, noise, and computation time (Abdi, 2010). Orthogonalized PLSR algorithms were performed on the calibration data with adulteration concentration as Y-variable. The performance of the PLSR model's calibration and prediction in the study were shown Table 1.

The model obtained from the reflectance spectra already has an outstanding performance with $R^2 > 0.90$. Model performance could be increased by log (1/R) transformation of reflectance spectra. However, the KM transformation of reflectance spectra yielded a lower model performance. The model obtained by raw spectra of log (1/R) and KM is also the model that has the best performance compared to pre-processed Log(1/R) and pre-processed KM model. Pre-processing of either Log(1/R) or KM spectra negatively impact the performance of the built PLSR model and yields a lower model performance.

Overall, reflectance spectra yielded a better average of model performance than log (1/R), and KM-transformed spectra. Reflectance spectra yielded R^2 of prediction ranging from 0.88 to 0.96, with an average R^2 of 0.92. Log(1/R) spectra yielded a bit lower R^2 of prediction ranging from 0.87 to 0.95, with an average R^2 of prediction of 0.91. A similar performance of reflectance and log (1/R) was also found by (Nicolai et al., 2007b). KM spectra model yielded the worst model performances with R^2 of prediction ranging from 0.82 to 0.93, with an average of 0.88. KM spectra yielding a poor model compared to pre-process, and other spectral transformations were also reported by (Vasques et al., 2008).

The best model performance from reflectance spectra was yielded by SGS pre-processed spectra. SGS pre-processed reflectance spectra have the highest R^2 and lowest RMSE of calibration and high prediction performance. With an R^2 prediction of 0.96, the model obtained could be used in most applications, including quality control (Williams & Norris, 2001). Figure 2 shows the best model's regression coefficient (B) from reflectance, KM, and log(1/R) spectra. Regression coefficient (B) can help explain which wavelength influences the model the most. Based on the regression coefficient (B)

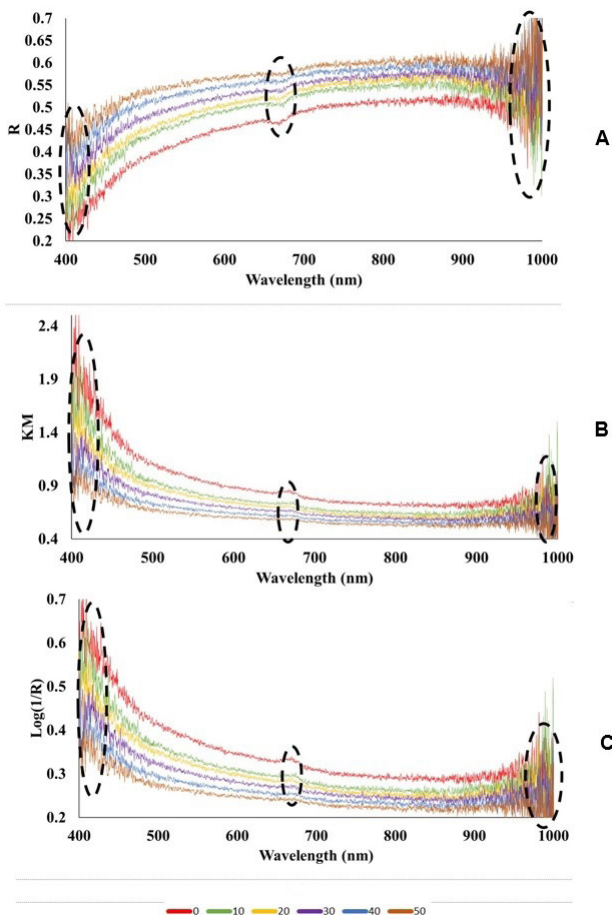
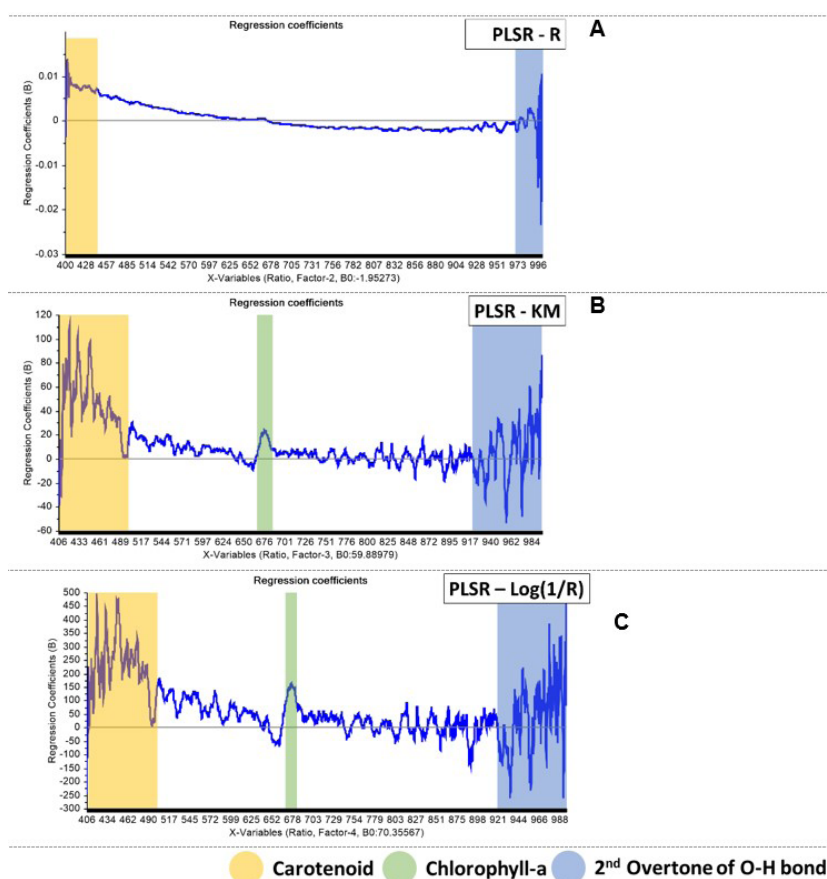


Figure 1. Adulterated samples differentiation with direct comparison of spectra obtained by different pre-processing data. Data was obtained with (A) Original Vis/NIR reflectance spectra, (B) Kubelka-Munk transformation spectra, and (C) Log(1/R) transformation spectra of adulterated brown rice.

Table 1. PLSR model performances.

| Pre-process technique | R | | | | KM | | | | Log(1/R) | | | |
|-----------------------|----------------|-------------|----------------|-------------|----------------|-------------|----------------|-------------|----------------|-------------|----------------|-------------|
| | C | | P | | C | | P | | C | | P | |
| | R ² | RMSE |
| Raw | 0.94 | 4.02 | 0.95 | 4.00 | 0.92 | 4.71 | 0.93 | 4.80 | 0.95 | 3.94 | 0.95 | 3.84 |
| SGS | 0.95 | 3.79 | 0.96 | 3.57 | 0.90 | 5.41 | 0.92 | 5.03 | 0.94 | 4.08 | 0.95 | 3.80 |
| AN | 0.94 | 4.11 | 0.96 | 3.53 | 0.87 | 5.99 | 0.93 | 4.74 | 0.90 | 5.28 | 0.89 | 5.74 |
| SNV | 0.87 | 5.97 | 0.88 | 5.96 | 0.83 | 7.03 | 0.86 | 6.62 | 0.87 | 6.05 | 0.87 | 6.23 |
| MSC | 0.87 | 6.01 | 0.88 | 6.01 | 0.82 | 7.08 | 0.86 | 6.66 | 0.87 | 6.10 | 0.87 | 6.30 |
| SGD 1st | 0.95 | 3.91 | 0.88 | 6.05 | 0.82 | 7.07 | 0.82 | 7.45 | 0.94 | 4.18 | 0.93 | 4.56 |
| Max | 0.95 | 6.01 | 0.96 | 6.05 | 0.92 | 7.08 | 0.93 | 7.45 | 0.95 | 6.10 | 0.95 | 6.30 |
| Min | 0.87 | 3.79 | 0.88 | 3.53 | 0.82 | 4.71 | 0.82 | 4.74 | 0.87 | 3.94 | 0.87 | 3.80 |
| Average | 0.92 | 4.63 | 0.92 | 4.85 | 0.86 | 6.21 | 0.88 | 5.88 | 0.91 | 4.94 | 0.91 | 5.08 |

Note: R = reflectance; KM = Kubelka-Mulk transformation; C = calibration; P = prediction; R² = coefficient determination; RMSE = root mean square error; SGS = Savitsky-Golay's smoothing; AN = area normalization; SNV = standard normal variate; MSC = multiple scatter correction; SGD = Savitsky-Golay's Derivative.

**Figure 2.** PLSR regression coefficient (B) using (A) SGS pre-processed reflectance spectra, (B) Raw KM spectra, (C) Raw Log(1/R) spectra.

shown in Figure 2, the three models were strongly influenced by carotenoid pigments on the wavelength 400-500 nm and the second overtone of the O-H bond stretching on the 915-1000 nm. Apart from the carotenoid and O-H bond wavelength, the regression coefficient (B) of KM and log (1/R) shows that these models are also influenced by chlorophyll-a at around 678 nm.

3.3 PCR model

Besides PLSR, in this study, we used PCR as a calibration method to connect multi variables of spectra with adulteration concentration. Like PLSR, PCR is a quantification-supervised analysis that works with two stages of analysis. First, dimension reduction of multivariable spectra into new variables (up to 20) called principal components (PCs). Second, linear regression

relates each PC score with the dependent variable (Vasques et al., 2008). Each PC will have its model performance, namely regression coefficient (R^2) and root mean square error (RMSE). PCs with the lowest RMSE and highest R^2 (max. 1) will be selected.

Table 2 shows the PCR model performance to predict adulteration in black rice flour. KM spectra yielded a model with the highest average of R^2 of prediction, which was 0.91, with R^2 of prediction ranging from 0.86 to 0.94. The average R^2 of the Log(1/R) model's predictions ranks second with a value of 0.87, ranging from 0.74 to 0.95. Reflectance spectra yielded a model with the lowest average R^2 with a value of 0.85, ranging from 0.48 to 0.96. Despite having a low average R^2 , reflectance

spectra yielded the best model with the highest R^2 of prediction and lowest RMSE, which were 0.96 and 3.42, respectively. The best model was obtained using reflectance spectra without pre-processing. This model could be considered a good model. With R^2 of 0.95, the model could be used for most applications, including quality control (Williams & Norris, 2001).

The regression coefficient (B) of the best reflectance, KM, and log(1/R) model is shown in Figure 3. Like PLSR models, the PCR model is influenced by carotenoids and second overtones of the O-H bond. Moreover, a weak chlorophyll- α peak also appears on the KM and log(1/R) models. The wavelength at around 930-1000 nm is the wavelength that contributes the most to the model prediction.

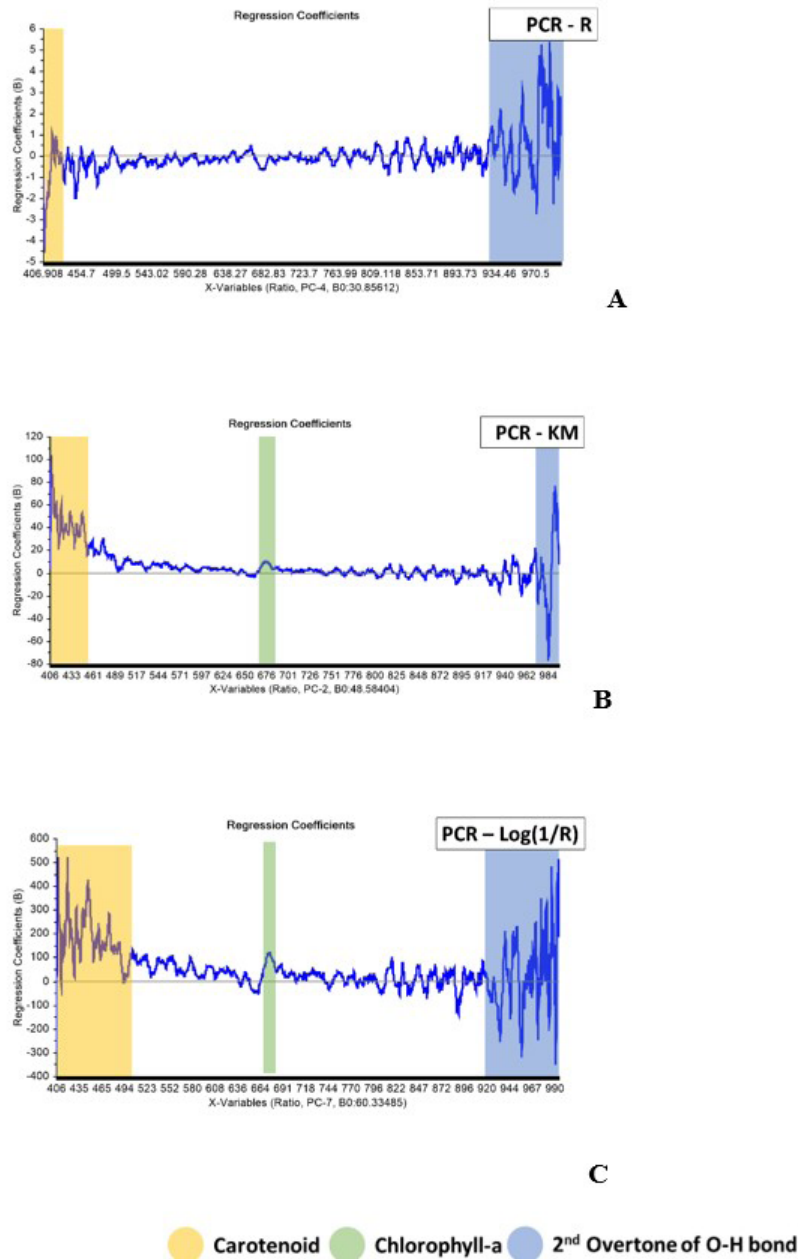


Figure 3. PCR regression coefficient (B) using (A) Raw reflectance spectra, (B) SGS pre-processed KM spectra, (C) SGS pre-processed Log(1/R) spectra.

Table 2. PLSR model performances.

| Pre-process technique | R | | | | KM | | | | Log(1/R) | | | |
|-----------------------|----------------|-------------|----------------|-------------|----------------|-------------|----------------|-------------|----------------|-------------|----------------|-------------|
| | C | | P | | C | | P | | C | | P | |
| | R ² | RMSE |
| Raw | 0.95 | 3.75 | 0.96 | 3.42 | 0.92 | 4.65 | 0.93 | 4.63 | 0.80 | 7.46 | 0.74 | 9.01 |
| SGS | 0.95 | 3.87 | 0.96 | 3.69 | 0.93 | 4.58 | 0.94 | 4.42 | 0.93 | 4.33 | 0.95 | 4.11 |
| AN | 0.94 | 4.17 | 0.96 | 3.59 | 0.88 | 5.88 | 0.93 | 4.70 | 0.85 | 6.47 | 0.90 | 5.62 |
| SNV | 0.84 | 6.65 | 0.88 | 6.07 | 0.93 | 4.54 | 0.87 | 6.44 | 0.83 | 6.84 | 0.87 | 6.34 |
| MSC | 0.84 | 6.69 | 0.88 | 6.10 | 0.92 | 4.74 | 0.86 | 6.55 | 0.83 | 6.90 | 0.87 | 6.39 |
| SGD 1st | 0.50 | 11.85 | 0.48 | 12.66 | 0.92 | 4.80 | 0.91 | 5.31 | 0.90 | 5.28 | 0.90 | 5.42 |
| Max | 0.95 | 11.85 | 0.96 | 12.66 | 0.93 | 5.88 | 0.94 | 6.55 | 0.93 | 7.46 | 0.95 | 9.01 |
| Min | 0.50 | 3.75 | 0.48 | 3.42 | 0.88 | 4.54 | 0.86 | 4.42 | 0.80 | 4.33 | 0.74 | 4.11 |
| Average | 0.84 | 6.16 | 0.85 | 5.92 | 0.92 | 4.86 | 0.91 | 5.34 | 0.86 | 6.21 | 0.87 | 6.15 |

Note: R = reflectance; KM = Kubelka-Munk transformation; C = calibration; P = prediction; R² = coefficient determination; RMSE = root mean square error; SGS = Savitsky-Golay's smoothing; AN = area normalization; SNV = standard normal variate; MSC = multiple scatter correction; SGD = Savitsky-Golay's Derivative.

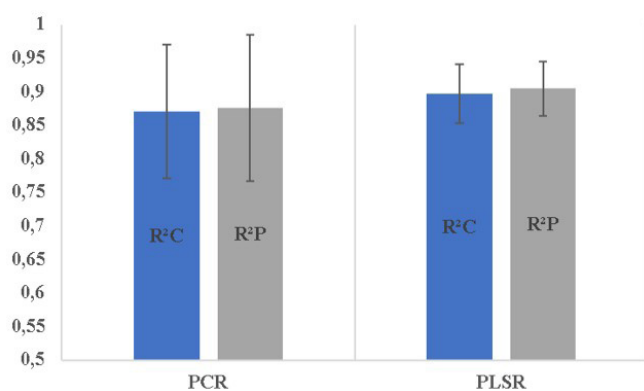


Figure 4. Overall average R² of PLSR and PC from reflectance, KM, and Log(1/R) model.

3.4 Comparison of PLSR and PCR model

To obtain the best model to predict adulteration of white rice flour in brown rice flour, performance of PLSR and PCR model were compared. Based on the result found, PLSR and PCR models have similar results. However, based on the overall average shown in Figure 4, PLSR models have slightly better performance than the PCR model. PLSR have a higher overall average R² of calibration and prediction compared to overall average R² of PCR. Moreover, based on the standard deviation of R², PCR models have a wider range of R² compared PLSR. The better performance of PLS is because PLS taking into account the dependent variable when forming new variables (PLS factor) of PLSR (Vasques et al., 2008). According to (Shao et al., 2007), PLSR did not include latent variables that are insignificant to the variance of quality parameters. However, with a prediction R² of 0.96, the best model from both methods PCR and PLSR has an outstanding performance. In addition, both models are influenced by the same wavelength, precisely the wavelengths associated with the stretching of carotenoids and OH bonds.

4 Conclusion

This article shows that reflectance spectra yielded model performances superior to KM and log (1/R) spectra. The best

model for both PLSR and PCR was acquired using reflectance spectra. The best model for PLSR was obtained using SGS pre-processing spectra, while the best model for PCR was obtained using raw reflectance spectra. PLSR and PCR produce the optimal model with an identical R² value of 0.96. However, based on the overall average of R² of prediction, PLSR is superior to PCR. Nevertheless, it is proven that reflectance spectra of visible near-infrared spectrometers combined with either PLSR or PCR can predict the adulteration of white rice flour in brown rice flour.

Conflict of interest

The authors declare no conflict of interest.

Acknowledgements

We are very much thankful for the Vis-NIR miniature spectrometer facility, Flame-T-VIS-NIR Ocean Optics, Department of Agricultural and Biosystems Engineering, Faculty of Agricultural Technology, Universitas Gadjah Mada, Indonesia.

References

- Abdi, H. (2010). Partial least squares regression and projection on latent structure regression (PLS Regression). *Wiley Interdisciplinary Reviews: Computational Statistics*, 2(1), 97-106. <http://dx.doi.org/10.1002/wics.51>.
- Chen, Q., Zhao, J., Zhang, H., & Wang, X. (2006). Feasibility study on qualitative and quantitative analysis in tea by near infrared spectroscopy with multivariate calibration. *Analytica Chimica Acta*, 572(1), 77-84. <http://dx.doi.org/10.1016/j.aca.2006.05.007>. PMID:17723463.
- Cortés, V., Ortiz, C., Aleixos, N., Blasco, J., Cubero, S., & Talens, P. (2016). A new internal quality index for mango and its prediction by external visible and near-infrared reflection spectroscopy. *Postharvest Biology and Technology*, 118, 148-158. <http://dx.doi.org/10.1016/j.postharvbio.2016.04.011>.
- Cruz, J. F. O. (2007). Classification of chocolate according to its cocoa percentage by using Terahertz time- domain spectroscopy. *Food Science and Technology*, 8, 587-590.
- Fernández-Novales, J., Garde-Cerdán, T., Tardáguila, J., Gutiérrez-Gamboa, G., Pérez-Álvarez, E. P., & Diago, M. P. (2019). Assessment of amino

- acids and total soluble solids in intact grape berries using contactless Vis and NIR spectroscopy during ripening. *Talanta*, 199, 244-253. <http://dx.doi.org/10.1016/j.talanta.2019.02.037>. PMID:30952253.
- Guo, Z., Huang, W., Peng, Y., Chen, Q., Ouyang, Q., & Zhao, J. (2016). Color compensation and comparison of shortwave near infrared and long wave near infrared spectroscopy for determination of soluble solids content of "Fuji" apple. *Postharvest Biology and Technology*, 115, 81-90. <http://dx.doi.org/10.1016/j.postharvbio.2015.12.027>.
- Jaiswal, P., Jha, S. N., Kaur, P. P., Bhardwaj, R., Singh, A. K., & Wadhawan, V. (2014). Prediction of textural attributes using color values of banana (*Musa sapientum*) during ripening. *Journal of Food Science and Technology*, 51(6), 1179-1184. <http://dx.doi.org/10.1007/s13197-012-0614-2>. PMID:24876653.
- Jie, D., Xie, L., Rao, X., & Ying, Y. (2014). Using visible and near infrared diffuse transmittance technique to predict soluble solids content of watermelon in an on-line detection system. *Postharvest Biology and Technology*, 90, 1-6. <http://dx.doi.org/10.1016/j.postharvbio.2013.11.009>.
- Juhász, R., Gergely, S., Gelencsér, T., & Salgó, A. (2005). Relationship between NIR spectra and RVA parameters during wheat germination. *Cereal Chemistry*, 82(5), 488-493. <http://dx.doi.org/10.1094/CC-82-0488>.
- Laborde, A., Puig-Castellví, F., Jouan-Rimbaud Bouveresse, D., Eveleigh, L., Cordella, C., & Jaillais, B. (2021). Detection of chocolate powder adulteration with peanut using near-infrared hyperspectral imaging and Multivariate Curve Resolution. *Food Control*, 119, 107454. <http://dx.doi.org/10.1016/j.foodcont.2020.107454>.
- Lamberts, L., & Delcour, J. A. (2008). Carotenoids in raw and parboiled brown and milled rice. *Journal of Agricultural and Food Chemistry*, 56(24), 11914-11919. <http://dx.doi.org/10.1021/jf802613c>. PMID:19012405.
- Lichtenthaler, H. K., & Buschmann, C. (2001). Chlorophylls and carotenoids: measurement and characterization by UV-VIS spectroscopy. *Current Protocols in Food Analytical Chemistry*, 1(1), F4.3.1, 8. <http://dx.doi.org/10.1002/0471142913.faf0403s01>.
- Masithoh, R. E., Amanah, H. Z., & Cho, B. K. (2020a). Application of fourier transform near-infrared (FT-NIR) and fourier transform infrared (FT-IR) spectroscopy coupled with wavelength selection for fast discrimination of similar color of tuber flours. *Indonesian Journal of Chemistry*, 20(3), 680-687. <http://dx.doi.org/10.22146/ijc.48092>.
- Masithoh, R. E., Lohumi, S., Yoon, W. S., Amanah, H. Z., & Cho, B. K. (2020b). Development of multi-product calibration models of various root and tuber powders by fourier transform near infra-red (FT-NIR) spectroscopy for the quantification of polysaccharide contents. *Heliyon*, 6(10), e05099. <http://dx.doi.org/10.1016/j.heliyon.2020.e05099>. PMID:33134571.
- Masithoh, R. E., Roosmayanti, F., Rismiwindira, K., & Pahlawan, M. F. R. (2022). Detection of palm sugar adulteration by Fourier Transform Near-Infrared (FT-NIR) and Fourier Transform Infrared (FT-IR) spectroscopy. *Sugar Tech*, 24(3), 920-929. <http://dx.doi.org/10.1007/s12355-021-01058-3>.
- Mishra, P., Biancolillo, A., Roger, J. M., Marini, F., & Rutledge, D. N. (2020). New data preprocessing trends based on ensemble of multiple preprocessing techniques. *Trends in Analytical Chemistry*, 132, 116045. <http://dx.doi.org/10.1016/j.trac.2020.116045>.
- Mishra, P., Rutledge, D. N., Roger, J. M., Wali, K., & Khan, H. A. (2021). Chemometric pre-processing can negatively affect the performance of near-infrared spectroscopy models for fruit quality prediction. *Talanta*, 229, 122303. <http://dx.doi.org/10.1016/j.talanta.2021.122303>. PMID:33838766.
- Nicolai, B. M., Beullens, K., Bobelyn, E., Peirs, A., Saeys, W., Theron, K. I., & Lammertyn, J. (2007a). Nondestructive measurement of fruit and vegetable quality by means of NIR spectroscopy: a review. *Postharvest Biology and Technology*, 46(2), 99-118. <http://dx.doi.org/10.1016/j.postharvbio.2007.06.024>.
- Nicolai, B. M., Theron, K. I., & Lammertyn, J. (2007b). Kernel PLS regression on wavelet transformed NIR spectra for prediction of sugar content of apple. *Chemometrics and Intelligent Laboratory Systems*, 85(2), 243-252. <http://dx.doi.org/10.1016/j.chemolab.2006.07.001>.
- Nielsen, S. S. (2017). *Food analysis* (5th ed.). Cham: Springer. <http://dx.doi.org/10.1007/978-3-319-45776-5>.
- Quelal-Vásconez, M. A., Lerma-García, M. J., Pérez-Esteve, É., Arnau-Bonachera, A., Barat, J. M., & Talens, P. (2019). Fast detection of cocoa shell in cocoa powders by near infrared spectroscopy and multivariate analysis. *Food Control*, 99, 68-72. <http://dx.doi.org/10.1016/j.foodcont.2018.12.028>.
- Quelal-Vásconez, M. A., Pérez-Esteve, É., Arnau-Bonachera, A., Barat, J. M., & Talens, P. (2018). Rapid fraud detection of cocoa powder with carob flour using near infrared spectroscopy. *Food Control*, 92, 183-189. <http://dx.doi.org/10.1016/j.foodcont.2018.05.001>.
- Rahmawati, L., Masithoh, R. E., Pahlawan, M. F. R., & Hariadi, H. (2022). Detection of Encapsulant addition in butterfly-pea (*Clitoria ternatea* L.) extract powder using visible-near infrared spectroscopy and chemometrics analysis. *Open Agriculture*, 7(1), 711-723. <http://dx.doi.org/10.1515/opag-2022-0135>.
- Rismiwindira, K., Roosmayanti, F., Pahlawan, M. F. R., & Masithoh, R. E. (2021). Application of Fourier Transform Near-Infrared (FT-NIR) spectroscopy for detection of adulteration in palm sugar. *IOP Conference Series. Earth and Environmental Science*, 653(1), 012122. <http://dx.doi.org/10.1088/1755-1315/653/1/012122>.
- Rodríguez, S. D., Rolandelli, G., & Buera, M. P. (2019). Detection of quinoa flour adulteration by means of FT-MIR spectroscopy combined with chemometric methods. *Food Chemistry*, 274, 392-401. <http://dx.doi.org/10.1016/j.foodchem.2018.08.140>. PMID:30372956.
- Roosmayanti, F., Rismiwindira, K., & Masithoh, R. E. (2021). Detection of coconut (*Cocos nucifera*) sugar adulteration in palm (*Arenga pinnata* Merrill) sugar by Fourier Transform Infrared (FT-IR) spectroscopy. *Food Research*, 5(S2), 31-36. [http://dx.doi.org/10.26656/fr.2017.5\(S2\).013](http://dx.doi.org/10.26656/fr.2017.5(S2).013).
- Santos, C. A. T., Lopo, M., Páscoa, R. N. M. J., & Lopes, J. A. (2013). A review on the applications of portable near-infrared spectrometers in the agro-food industry. *Applied Spectroscopy*, 67(11), 1215-1233. <http://dx.doi.org/10.1366/13-07228>. PMID:24160873.
- Schaare, P. N., & Fraser, D. G. (2000). Comparison of reflectance, interactance and transmission modes of visible-near infrared spectroscopy for measuring internal properties of kiwifruit (*Actinidia chinensis*). *Postharvest Biology and Technology*, 20(2), 175-184. [http://dx.doi.org/10.1016/S0925-5214\(00\)00130-7](http://dx.doi.org/10.1016/S0925-5214(00)00130-7).
- Schoot, M., Kapper, C., van Kollenburg, G. H., Postma, G. J., van Kessel, G., Buydens, L. M. C., & Jansen, J. J. (2020). Investigating the need for preprocessing of near-infrared spectroscopic data as a function of sample size. *Chemometrics and Intelligent Laboratory Systems*, 204, 104105. <http://dx.doi.org/10.1016/j.chemolab.2020.104105>.
- Shao, Y., He, Y., Gómez, A. H., Pereir, A. G., Qiu, Z., & Zhang, Y. (2007). Visible/near infrared spectrometric technique for nondestructive assessment of tomato "Heatwave" (*Lycopersicon esculentum*) quality characteristics. *Journal of Food Engineering*, 81(4), 672-678. <http://dx.doi.org/10.1016/j.jfoodeng.2006.12.026>.
- van der Meer, F. (2018). Near-infrared laboratory spectroscopy of mineral chemistry: a review. *International Journal of Applied Earth Observation and Geoinformation*, 65, 71-78. <http://dx.doi.org/10.1016/j.jag.2017.10.004>.

- Vasques, G. M., Grunwald, S., & Sickman, J. O. (2008). Comparison of multivariate methods for inferential modeling of soil carbon using visible/near-infrared spectra. *Geoderma*, 146(1–2), 14-25. <http://dx.doi.org/10.1016/j.geoderma.2008.04.007>.
- Veselá, A., Barros, A. S., Synytsya, A., Delgadillo, I., Čopíková, J., & Coimbra, M. A. (2007). Infrared spectroscopy and outer product analysis for quantification of fat, nitrogen, and moisture of cocoa powder. *Analytica Chimica Acta*, 601(1), 77-86. <http://dx.doi.org/10.1016/j.aca.2007.08.039>. PMID:17904472.
- Walsh, K. B., McGlone, V. A., & Han, D. H. (2020). The uses of near infra-red spectroscopy in postharvest decision support: a review. *Postharvest Biology and Technology*, 163, 111139. <http://dx.doi.org/10.1016/j.postharvbio.2020.111139>.
- Williams, P., & Norris, K. (2001). *Near-infrared technology in the agricultural and food industries*. St. Paul: American Association of Cereal Chemists.
- Wu, D., Feng, S., & He, Y. (2008). Short-wave near-infrared spectroscopy of milk powder for brand identification and component analysis. *Journal of Dairy Science*, 91(3), 939-949. <http://dx.doi.org/10.3168/jds.2007-0640>. PMID:18292249.
- Xie, L., Ying, Y., & Ying, T. (2009). Rapid determination of ethylene content in tomatoes using visible and short-wave near-infrared spectroscopy and wavelength selection. *Chemometrics and Intelligent Laboratory Systems*, 97(2), 141-145. <http://dx.doi.org/10.1016/j.chemolab.2009.03.005>.
- Xu, L., Yan, S. M., Cai, C. B., & Yu, X. P. (2013). Untargeted detection of illegal adulterations in Chinese Glutinous Rice Flour (GRF) by NIR spectroscopy and chemometrics: specificity of detection improved by reducing unnecessary variations. *Food Analytical Methods*, 6(6), 1568-1575. <http://dx.doi.org/10.1007/s12161-013-9575-y>.
- Zhang, Y., Wang, J., Luo, H., Yang, J., Wu, X., Wu, Q., & Zhong, Y. (2023). Rapid prediction of Yongchuan Xiuya tea quality by using near infrared spectroscopy coupled with chemometric methods. *Food Science and Technology*, 43, e101122. <http://dx.doi.org/10.1590/fst.101122>.
- Zhou, M., Long, T., Zhao, Z., Chen, J., Wu, Q., Wang, Y., & Zou, Z. (2023). Honey quality detection based on near-infrared spectroscopy. *Food Science and Technology*, 43, e98822. <http://dx.doi.org/10.1590/fst.98822>.